On *u-d* Quark Coulomb Origin of Nuclear Force

Abstract

The origin of nuclear force is assigned to Coulomb interactions between quarks, *u* and *d*, in neighbouring nucleons, replacing the current unspecified "residual" strong interaction assignment. The deuteron binding energy is correctly estimated using quasi-classical models for nucleons based upon SSI, the scalar strong interaction hadron theory. The next lightest nuclei are analogously treated. The Coulomb binding energies depend upon the small, in principle observable, internucleon distances between such *u* and *d* quarks whose positions in their respective host nucleons however depend upon intranucleon strong *u* - *d* potential that span over larger hidden distances.

Keywords: scalar strong interaction hadron theory SSI, nuclear binding energy, interquark Coulomb potential, quasi-classical nucleon model, nucleon "rod"

1. INTRODUCTION

1.1 Standard Model and Its Problems

The current mainstream elementary particle theory, the half century old standard model SM [1], [2 Standard Model], has not been proven to confine quarks and has failed to account forhadron spectra as well as dark matter and darkenergy. SM further requires the existence of a Higgs boson with isospin ≥1/ 2. The Higgs-like boson found in 2012 [3] however has an isospin compatible with 0 but not shown to be ≥1/2; it has been assigned to a W^+W^- bound state in SSI.

This status is a far cry from that of quantum mechanics. Within three decades after its inception in the 1920's, most of the atomic phenomena have been accounted for. The basic equation of motion in this theory is Dirac's equation for an electron. The Dirac wave function has four components, two large and two small, suitable for transition into nonrelativistic classical mechanics in the low energy limit, where the two large components dominate.

In SM and QCD (quantum chromodynamics), the Dirac equation has been adopted also for quarks. However, quarks are, contrary to electron, not visible and can be relativistic. So, the two large and two small components division of the Dirac wave function is not suitable for relativistic quarks. This is evident from the fact that the Dirac equation is not manifestly Lorentz covariant. The four component Dirac wave functions do not constitute a basis vector that generates representations of the Lorentz group. For quarks, therefore, manifestly Lorentz covariant equations are called for.

Furthermore, the quarks are assumed to interact strongly via "color vectorial" interactions. Thisappears to be incompatible with meson-nucleon and nucleon-nucleon scattering data which suggest that such strong interactions are scalar.

These problems underlie that nuclear binding energy, in the absence of a basic theory for nucleons, has been treated bythe empirical shell model [2 Nuclear shell Model]. It is conjectured that the strong interaction that hold together the quarks has some "residual" effect that makes up the internucleon binding energies. This residual effect has been criticized to be "vague" [2], justifiably so in view of the status of SM,

1.2 Scalar Strong Interaction Hadron Theory SSI [4-6]

In SSI, the Dirac equation has been transformed into the manifestly Lorentz covariant van der Waerden equations. The four component Dirac wave function has been transformed into two Weyl spinors, which are basis vectors generating the fundamental representation of the Lorentz group, the SL(2C) (SpecialLinear Groupof Rank 2Complex) group. Further, the quarks interact via scalar interaction.Although these quark equations differ from those of QCD in SM, they merge into each other at high energies [5, 6 Ch. 14].

The SSI equations of motion for mesons and baryons [4] have subsequently led to many results collected in [5, 6].

A purpose of this paper is to specify the above-mentioned "residual" effect in the framework of SSI which also offers a different strong interquark interaction from the SM one.
In Sec. 2,nuclear binding energy is assigned to Coulombattraction between *u* and *d* quarks inneighbouring nucleons. Representation of a nucleon is simplified to a quasi-classical "rod" with quarks onits ends.In Sec. 3, this model is applied to the binding energies of two, three and four nucleon nuclei.In Sec. 4, heavier nuclei scenarios are closely connected to the invisible nature of quarks. For reference, some of the formulae in [4-6] are reproduced in the Appendix.

2. STRONG INTERACTION*u* - *d*AND "RESIDUAL" COULOMB ATTRACTION

2.1Scalar Strong Interaction*u* - *d*

In SSI, the *u* and *d* quarks interact strongly via the potential $V_s(r)$ given in (A18) and plotted in Figure A2. The magnitude of V_s is GeV and it increases with the*u*-*d* separation so that even a residual part of 1%can be> 9 MeV, the upper limitof binding energy per nucleon in nuclei, and is too big for those in the lightest nuclei.
More basically, V_s acts in the "hidden" relative space $\underline{x}$ between *u* and *d*in a nucleon and is not visible in the laboratory space $\underline{X}$ in which the binding energiesare observable. In this way, nature guarantees that a nucleon is always bound and inaccessible to direct outer forces in laboratory space $\underline{X}$that may tend to break it apart so as to violate baryon number conservation and threaten the persistence of the universe.

2.2*u* -*d* Internucleon Coulomb Attraction as Origin of "Residual"Nuclear Force

At the end of the Appendix, it is pointed out that the strong interaction results there are independent of the charges of the quarks, as if they were "switched off". This is so because the *u* and *d* quarks are separated by a distance of about 3.05 fm (A17) in the hidden relative space $\underline{x}$. But Coulomb interaction is in principle observable and takes place in the laboratory frame$\underline{X}$but may not be so in the invisible $\underline{x}$ space. Thus, the assignmentisthat the*u* and *d* quarks inside the same nucleon interact via strong interaction $V_s(r)$only. While Coulomb interaction takes place between*u* and *d* quarks in different nucleons, separated in the laboratory frame $\underline{X}$.

As a quark charge is attached to its host quark, its Coulomb interaction accompanies the strong interaction V_s associated with the host quark and may be considered as some"residual" interaction.Since such Coulomb interactions take place between nucleons in $\underline{X}$ space, they may provide the origin of nuclear binding energy. This will be investigated in the remainder of this paper.

2.3Quasi-classical Nucleon "Rod" Model

Nuclear binding involves at least two nucleons constituting a four-body problem, which is beyond the scope of the present work. Here, it will be estimated heuristically using simplified quasi-classical models based upon the quantum mechanical SSI treatment summarized in the Appendix.
In this approach, the detailed distributions of the quark clouds,$g(r)$ and $f(r)$ in Figure A1, are replaced apoint *u* quark and a point *dd* diquark connected by a "rod" of length r_a = 3.05 fm (A17). This invisible neutron rod is part of the hidden space coordinate *x* in (A4) and is illustrated in the upper figure in Figure 1, where the neutron coordinate $\underline{X}_n$ lies in the observable laboratory space *X* in (A4) and in the middle of this rod, corresponding to a_m=1/2 in (A6).
As was pointed out at the end of the Appendix, the neutron results there also hold approximately for the proton. Here, however, the proton charge is an observable quantity in *X* space and is illustrated by the large circle in Figure1. The laboratory coordinate $\underline{X}_p$ of the proton lies in the middle of this circle.
Theoretically, the simplest assignment is that this circle represents a solid spherewith radiusR_{p0} containing a charge *e* with a constant charge density inside it and 0 outside it. In this way, only one parameter R_{p0} enters the theory. Let the distance from the center of this sphere be R_p, this sphere generates a potential $\propto R_p^2$inside it and is a constant outside it.

The proton charge radius given by Particle Data Group, PDG, comes mostly from e-p scattering. The reported value R_{prms} = 0.831 fm is the root mean square of many measurements. Adopting the conventionalnormal distribution, this value implies

$$R_{prms} = (\int dR_p \times R_p^3 \times exp(-R_p^2/R_{p0}^2)) / (\int dR_p \times R_p^2 \times exp(-R_p^2/R_{p0}^2)) = 0.831 \text{ fm} \quad (2.1a)$$

$$R_{p0} = 2/\sqrt{\pi} \times 0.831 \text{ fm} = 0.736 \text{ fm} \quad (2.1b)$$

which is an analog to the "rod" length (A17) in the hidden space.

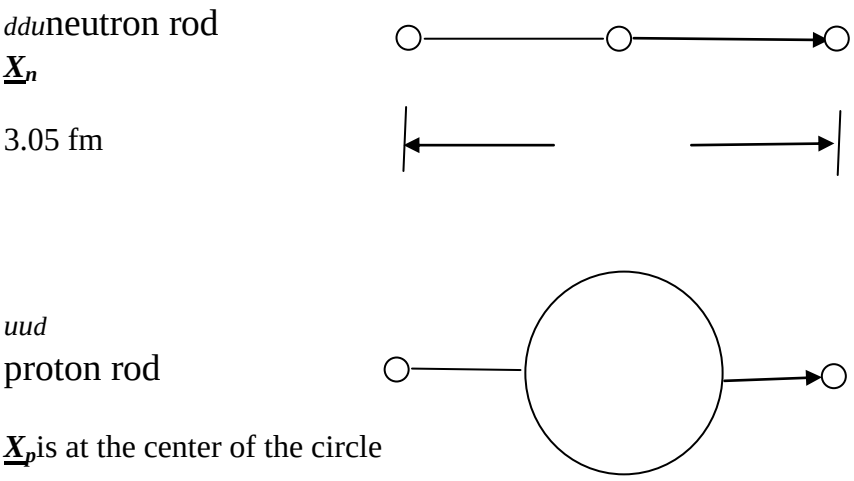

Figure 1. Quasi-classical illustration of a neutron rod and a proton rod.
A rod represents the diquark-quark distance vector $\underline{x}$ in the hidden, invisible relative space and is straight by definition or rigid. The large circle represents the proton charge sphere with effective radius $R_{p0}\approx 0.74$ fm in the visible laboratory space. The small circle in the middle of the neutron rod has an unknown, small diameter because the neutron has no charge. *u* and *d* stand for the up and down quark flavors. The arrows refer to the spin directions. The only directions available are those along the rods. The quarks in the diquarks *uu* and *dd* have opposite spins by Pauli's principle so that the ground state diquark has spin 0. The nucleon spin is that of the unpaired quark. The laboratory coordinate of the neutron $\underline{X}_n$ is located at the center of the neutron rod. The laboratory coordinate of the proton $\underline{X}_p$is located at the center of the large circle representing the size of the proton charge sphere.

Application of this "rod" model to hydrogen gas in cosmology with $a_m\neq 1/2$ in (A6) has led to successful predictions beneath (A6).

3. APPLICATION TOBINDING ENERGIES OF LIGHTEST NUCLEI

3.1 Deuteron ^2H

Let a proton *p* approach a neutron*n* from a distance. There is no attractive force between them in the laboratory frame because*n* has no charge. In Figure1, however, it can be seen that the *uu* diquark in *p* can attract the *dd* diquark in *n*. Such attraction moves *p* closer to *n*.To form a ^2H from them, both rods must be parallel so that their spins add up to 1. The maximum attraction is achieved if $|\underline{X}_n - \underline{X}_p|$ is a minimum. As the neutron at $\underline{X}_n$ cannot occupy the same space occupied by *p* in the laboratory frame $\underline{X}$, it can at best lie just outside the charge sphere of *p*, as is illustrated in Figure 2 This is equivalent to moving the neutron rod to just beneath the proton rod in Figure 2Any lateral shift of the rods relative to each other will increase the *u* to *d* distance and reduce their binding energy.

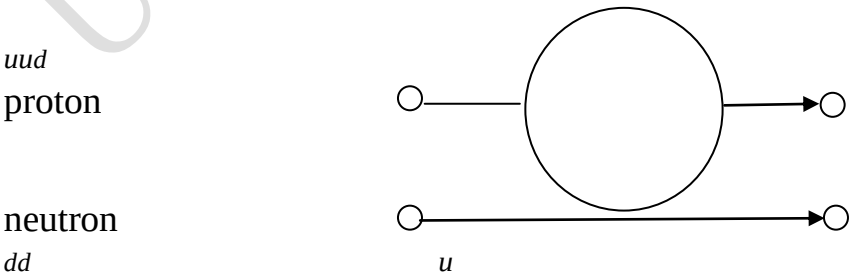

Figure 2Illustration of the quark structure of a deuteron employing the nucleon rods in Figure 2. The arrows give the spin direction. The distance between the rods is at least the charge radiusR_{p0}(2.1b) of the proton since both nucleons cannot occupy the same space in the observable laboratory space $\underline{X}$.

The binding energy between *uu* and *dd* and *d* and *u* according to Figure 3is then

$$E_{2H} = -\frac{q_{uu}\, q_{dd} + q_d q_u}{R_{p0}} = \frac{10e^2}{9R_{p0}} = 2.174 \text{ MeV} \qquad (3.1)$$

where the quark charges $q_u = 2e/3$, $q_d = -e/3$ and (2.1b) have been consulted. The *uu* diquark and the *u* quark are 4.26 times farther apart andthe interpretation is that interaction between them is forbidden by Pauli´s principle. The same holds for *dd* and *d*. (3.1) is 2.3% smaller than the measured PDG value 2.2245 MeV. These values are rather close, noting that the actual *u-d* interaction is quantum mechanical involving charge clouds rather than point charges in the rod model here. Such binding energies are of the magnitude of the proton electromagnetic self-energy $\boldsymbol{e}^2/R_{p0} \approx 1.96$ MeV, indicating their Coulomb nature. They are ~0.2% of the proton mass and appear to be too small to be any "residual" strong potential like $V_s(r)$ in Figure A2.

Conceptually, note that the observable laboratory *p-n* or rod separation $R_{p0} \approx 0.74$ fm is smaller than the invisible rod length $r_a = 3.05$ fm, which does not "compete" for space in the visible laboratory frame.

Another combination of the *p* and *n* rods is to turn the neutron rod 180° around its center at $\underline{X}_n$in Figure 3In this configuration, *uu* from *p* and the *u* from *n* are grouped together, repulse each other classically and violate Pauli´s principle quantum mechanically. The same holds for *dd* and *d* at the opposite end of the rods. Such spin 0 deuteron can therefore not exist, in agreement with data.

3.2 Dineutron ^2n

This case is complicated bythat the two participating neutrons are identical. The configuration of Figure 3below corresponds to the spin 0 deuteron case in the last paragraph, with the difference that there is no charge sphere that keeps both rods apart so they can get very close.

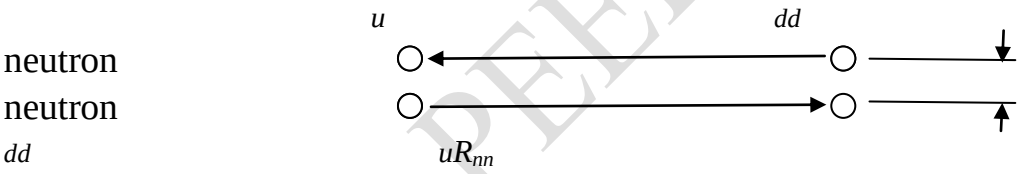

Figure 3. Illustration of the quark structure of a spin 0 dineutron.

The rod spacing R_{nn}may however not be 0. For small R_{nn}, a*u* quark at one end of a rod is so close to the*d*quark of the other neutron so that it may "abandon" its companion*d* quark far away on the same rod and tends to form a new neutron with the nearest*d* quark from the other neutron. In this case, Figure A2 and (A18) show that $R_{nn} > 0.288$ fm due to the large repulsive potential at smaller*u-d* separations.

However, such a smallR_n may even not be reachable because Figure A2 shows that a strong attractivepotential well is present in the 0.288 fm < $R_n \lessapprox 2$ fm region. Such a scenario implies a actually weaker *n-n* Coulombbonding. This is supported by that *n-p* pairs dominate over *n-n* pairs in heavier nuclei.

Here,however, only a lower limit of $R_n > 0.288$ fm will be set so thatthe upper limit of the spin0 dineutron binding energyis

$$E_{nn} < -\frac{2q_{dd}\, q_u}{R_{nn}} = \frac{8e^2}{9R_{p0}} = 4.94 \text{ MeV} \qquad (3.2)$$

Dineutron has been first observed a decade ago in ^{16}Be decay [7] but its binding energy has not been measured.

The third member in the two-nucleon system, the diproton *pp*, can be treated in an analogous manner. Neither the singlet nor the triplet *pp* is bound, as expected.

3.3 Tritium ^3H

Next, turn to the three body ^3H. The configuration in Figure 3 is achieved by adding a neutron to the deuteron in Figure 1 or a proton to the dineutron in Figure 3.

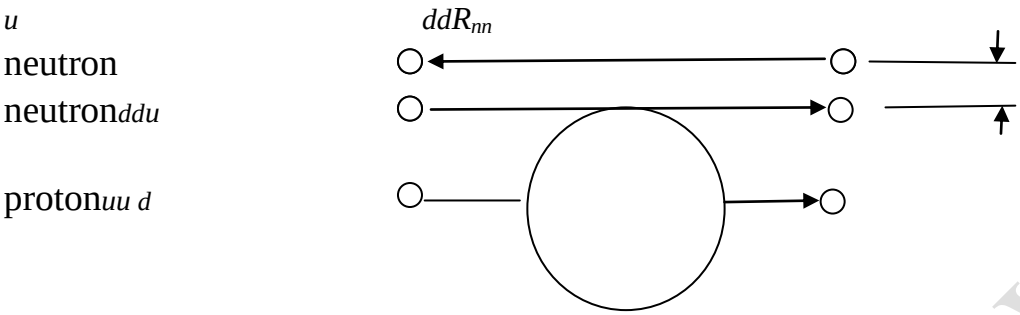

Figure 4Illustration of the quark structure of tritium.

The binding energy is simply the sum of (3.1) and (3.2),

$$E_{3H} = E_{2n} + E_{2H} < 7.11\ \text{MeV} < 8.48\ \text{MeV}\ \ (\text{PDG data}) \tag{3.3}$$

which is of the same magnitude as data but definitely smaller. Note that the interaction of the *u* quark in the top neutron with the *uu* diquark in the proton is forbidden by Pauli's principle. The same holds for that between the *dd* diquark in the top neutron and the *d* quark in the proton.

It is also possible to move the upper neutron rod to tangent the proton charge sphere from below. In this case, $E_{3H} = 2E_{2H} = 4.35$ MeV, still smaller than data.

This binding is a 3-body problem, but (3.3) only gives the sum of all three of possible 2-body binding energies. Genuine 3-body contribution is unknown.

3.4. Helium-3 ^3He

The configuration in Figure.4 can be obtained by adding a proton rod with opposite spin to the deuteron in Figure 1.

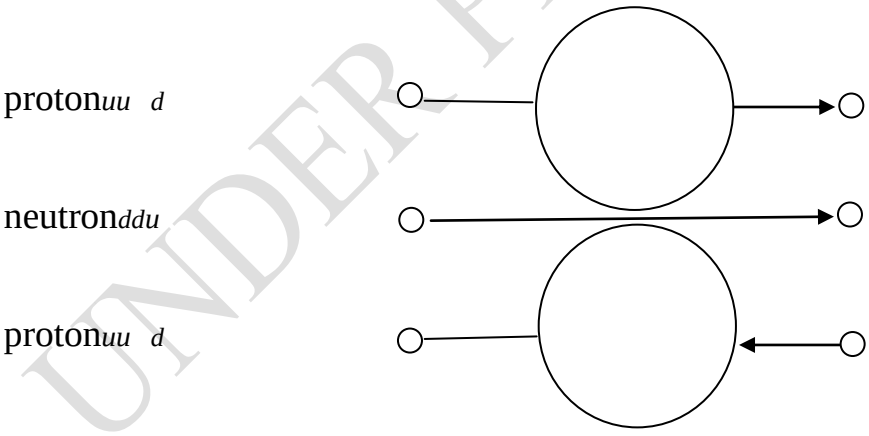

Figure 5. Illustration of the quark structure of helium-3.

In this case, the interpretation is that the fractional charges reside with the quarks at the ends of the rods; the two large spheres contain no charge to push them away from each other. On the other hand, when the charge of this ^3He is being measured, these quark charges will "rush" into these spheres to become measurable integer charges.

Analogous to the case in Figure 3,interaction between the two *uu* diquarks is forbidden by Pauli´s principle. The binding energy is simply twice the value of (3.1) minus a small energy of 0.1087 MeV due to the repulsion of the two *d* quarks,

$E_{He3} = 2E_{2H}$.–0.1087 = 4.24 MeV < 7.718 MeV (PDG data)(3.4)

Similar to (3.3), this binding is also a 3-body problem. But (3.4) only gives the sum of all three of possible 2-bodybinding energies. Genuine 3-body contribution has been mentionedin [2].

3.5. Helium-4 ^4He

The quarks of the nuclei treated above all lie on one two-dimensional plane. This no longer possible for ^4He, as is illustrated in Figure 5.

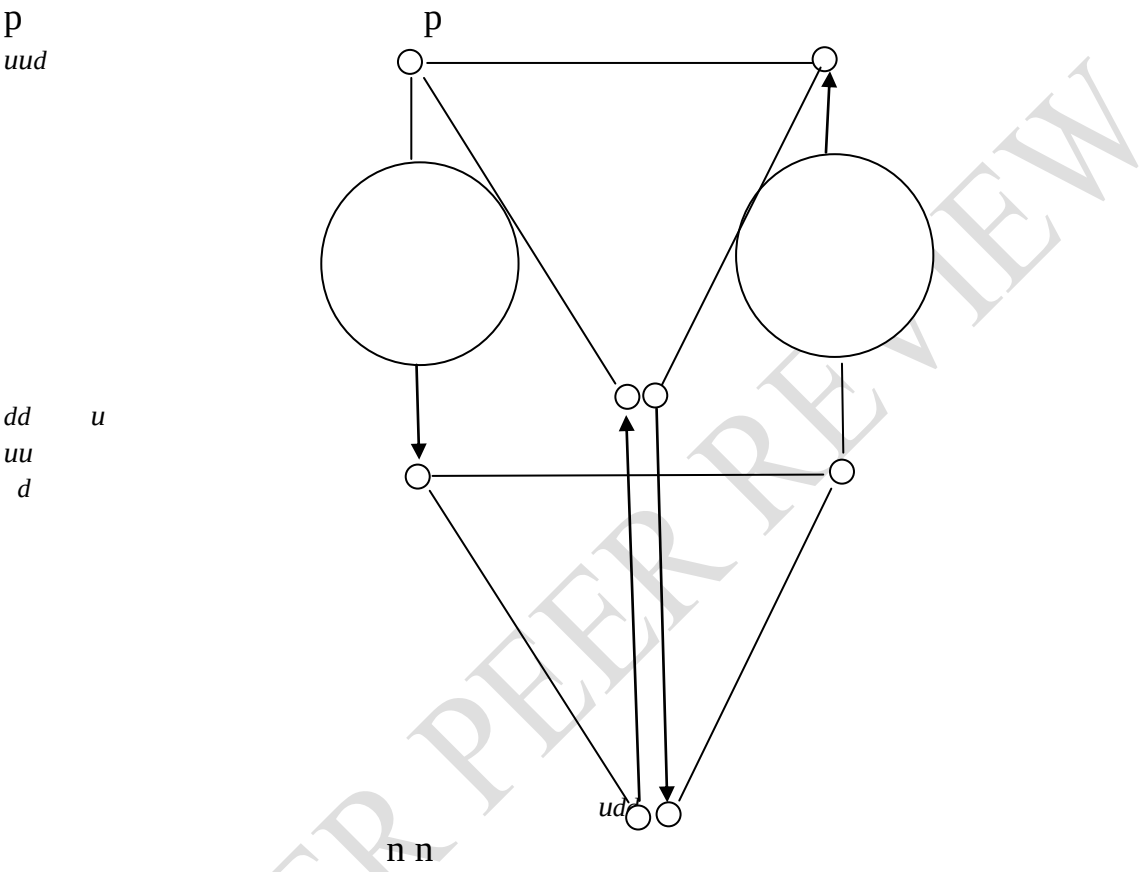

Figure 6. Illustration of the quark structure of helium-4.

To visualize this model, let a cube be put on a table in front of an observer. Let the square surface closest to the observer be narrowed down to a rectangle with the same height. Let the four corner lines connecting the top and bottom surfaces represent the four nucleon rods; the two of them on the front side represent two neutron rods with opposite spin, like those in Figure.2, and the two on the rear side two proton rods with opposite spin.

There are 20 internucleon "Coulomb legs" associated with Coulomb interaction energies between the quark charges at their ends, 4 on the top side,4 on the bottom side, 2 diagonal ones on each of the 4 side surfaces, and 4 diagonal ones between the top and bottom surfaces. The legs between *u* and *dd*in the neutrons are not shown because they are too short to be visible. Also, the protons are actually closer to each other so that their charge spheres actually touch each other, as in the Figure 4.

Contributions from the top and bottom surfaces dominate. The Coulomb attraction energybetween $p\downarrow$ and $n\uparrow$, where the arrows show the spin orientations in Figure 4,is the same as that in (3.1), The same holds for $p\uparrow$and $n\downarrow$. The contribution from$n\downarrow$ and $n\uparrow$ is the same as(3.2). The contribution from $p\downarrow$ and $p\uparrow$is

$$E_{pp} = -\frac{2q_{uu}\,q_d}{2R_{p0}} = \frac{2e^2}{9R_{p0}} = 0.435 \text{ MeV} \quad (3.5)$$

The sum of these four contributions is

$$2E_{2H} + E_{pp} + E_{nn} < 9.73\text{MeV} \quad (3.6)$$

The remaining 12 contributions are smaller because they involve the relatively larger rod length r_a= 3.05 fm (A17). Two of them violate Pauli´s principle and are left out. The remaining 10 contributions have been estimated to be 0.736 MeV. These leads to the estimated upper limit of helium-4 binding energy

$$E_{He4} < 9.73\text{MeV} + 0.736\text{MeV} = 10.49\ \text{MeV} < 28.3\ \text{MeV (PDG data)} \quad (3.7)$$

Analogous to (3.3, 4), this binding is a 4-body problem but (3.7) only gives the upper limit sum of allpossible 2-body binding energies. Genuine 3-body and 4-body contributions are ignored. The greater difference between the quasi-classical model result and data in (3.7), as compared to those in the 3-body nuclei results in (3.3) and (3.4), may indicate that genuine 4-body contribution is greater than genuine 3-body contributions, apart from departure from quantum mechanics.

4.HEAVIER NUCLEI SCENARIOS

4.1 "Quark Sharing" and Generation of Coulomb Legs

ConsiderFigure.5. The left *d* quark is the lower end of the p↓ rod as well as the left end of the so-created horizontal proton rod like Coulomb leg with the right *uu* at its right end. This *d* quark is thus "shared" between the real proton p↓and the created proton-like Coulomb leg that produces binding energy. In the configuration of ^4He in Figure.5, the four real nucleons produce 20 internucleon Coulomb legs, each contributing to binding energy, if not forbidden by Pauli´s principle.

Such situationsare expected to appear more frequently in heavier nuclei. In the present nucleon rod model of §2.3, the example of Figure.5 shows that a quark in a nucleon emanates6Coulomb legs connected to quarks in other nucleons. If this quark were surrounded by other nucleons in every direction, an additional 8 more Coulomb legs are in principle possible, totalling 14 Coulomb legs. Each such leg may be capable of generating binding energies. In the deuteron example in Figure.1, there are 4 such Coulomb legs generating a binding energy of 2.174 MeV in (3.1) or about 1 MeV per nucleon or 0.5 MeV per quark or diquark or Coulomb leg. Using these numbers, 14 Coulomb legs may generate up to 7 MeV binding energy per quark or 14 MeV per nucleon. This number is to be reduced by the number of legs violating the Pauli principle and double counting. In addition, genuine many-body interactions enter. Thus, the magnitude of such energies is comparable tothat of the maximal binding energy of ~9 MeVper nucleon for iron.

Thegenuine many-body interactions differ from those in a heavy atom, in which the large nucleus charge and mass dominate over those pertaining to the electrons. Perturbation calculations are applicable. Here, all the nucleons and quarks are more on equal footing. This more "democratic" scenario renders any theoretical treatment more complicated; there may not exist any small perturbative quantity.

Furthermore, the quasi-classical rod model above will become more insufficient under such circumstances and quantum mechanical aspects willvastly complicate the problems.

4.2 Hidden Space Overlapping.

The conceptual remark at the end of §3.1 leads to that the hidden volume of a nucleon $V_a = 4\pi(r_a/2)^3/3 \approx 15$ fm^3 is ≈3 times greater than the laboratory frame volume of a proton $\approx V_p = 4\pi(R_{p0})^3/3 \approx 5.2$ fm^3. These hold for each nucleon. In a heavy nucleus, each nucleon has its own "private" hidden V_a decoupled from the hidden V_a´s belonging to other nucleons. Thus, seen from their common laboratory frame, these V_a´s overlap but do not interfere with each other or lead to any observable, contradictory objection.

4.3 Coulomb Origin of "Residual" Strong Interaction

The nearly correct prediction of(3.1) for the deuteron binding energyand §4.1 suggest that nuclear force originates from Coulomb interactions between the different*u* and *d* quarks in different nucleons in nuclei and not from any "residual" strong force between the quarks in a nucleon. The word "residual" may be retained if it is reinterpreted asreferring to the much weaker internucleon, interquark Coulomb interactions in a nucleus.

If such “residual” force were of strong interaction nature, then fission of a nucleus may in principle alsolead to breaking apart aquark-diquark bond inside a nucleon giving rise to free quarks, contrary to experience. By keeping the strong interaction potential $V_s(r)$ in the hidden relative space inside a nucleon not accessible vialaboratory space forces, e. g. the Coulomb forces, the integrity of nucleon is guaranteed and not affected by such forces involved in fission processes. Such processes are driven by Coulomb repulsion between proton charge spheres (see Figure 1) and seek out locations where the interactions are weak and long range, here the Coulomb legs,and avoids locations where the interactions arestrong and short range; any eventual "residual” part of such has not been identified.

In the above, violation of Pauli´s principle was interpreted as no reaction but not repulsion between *uu* and *u*. This interpretation may depend upon the distances between these quarks and eventually also if the forces between them are perpendicular or parallel to the rod directions, as the charges can move along the rods. Further, Pauli´s principle, which holds for observable fermions, has not been proven to hold for invisible quarks. This point is not clear and the present interpretation is to be regarded as a working hypothesis in the present “rod model”.The actual Coulomb interactions in nuclei are so complex and involve quantum effects as well as the unknown, genuine many-quarkinteractionsso that they cannot be reached from the first principles SSI presently.

The strong potential $V_s(r)$ is about 10^2-10^3 times stronger than the Coulomb potentials in Sec. 3. Next comes the weak decay$d \rightarrow u + W^- \rightarrow u + e^- + \bar{\nu}_e$which is still weaker by a factor of ~10^5due to the large *W* mass.This decay, like the Coulomb case above, involves quark charges and takes place via the laboratory space *X*. It is responsible for the radioactive decays of nuclei isotopes and will be affected by the Coulomb interactions in Sec. 3. These points will further complicate the above scenario.

In conclusion, the present results revise our conceptionregarding the nature of nuclear force but do not affect the practical usefulness of theempirical shell and other models. In time, however, the Coulomb nature of nuclear force may enter into modifications and further developments of such models.

APPENDIX. EQUATIONS OF MOTION FOR NEUTRON IN SSI [4-6]

A.1 Covariant Equations ofMotion of Quark

Some of the formulae in Ch 2, 3, 9-12 for baryon in [5, 6] are reproduced here for reference.

A neutron contains 3 quarks. Let these be quarks *A*, *B* and *C*having masses m_A, m_B and m_C, flavors *d*, *u*and*d*,located atx_I, x_{II} and x_{III}, abbreviated by*I*,*II* and *III*, respectively.The van der Waerden spinor form of the Dirac equation for the *u* quark *B*interacting with the *d* quarks *A* and *C* via scalar interactionsV_{BA} and V_{BC}reads [5, 6 (9.1.2, 4b)]

$$\partial_{II}^{d\dot{e}}\chi_{B\dot{e}}(II) - i\big(V_{BC}(II)+V_{BA}(II)\big)\psi_B^d(II) = im_B\psi_B^d(II)$$
$$\partial_{II\dot{e}f}\psi_B^f(II) - i\big(V_{BC}(II)+V_{BA}(II)\big)\chi_{B\dot{e}}(II) = im_B\chi_{B\dot{e}}(II)$$
$$\Box_{II}\big(V_{BC}(II)+V_{BA}(II)\big) = \frac{1}{2}g_s^2\begin{pmatrix}\psi_C^g(II)\chi_{Cg}(II)+\psi_C^{\dot{g}}(II)\chi_{C\dot{g}}(II)+\\ +\psi_A^a(II)\chi_{Aa}(II)+\psi_A^{\dot{a}}(II)\chi_{A\dot{a}}(II)\end{pmatrix} \quad \text{(A1)}$$

Here, $\chi$and ψ are two component(Weyl) spinors [5, 6 Appendix B], [8] with their indices *d*, *e*, *f*…running from 1 to 2.$\partial_{II} = \partial/\partial x_{II}$. g_s is the strong coupling constant. The *V´s* are scalar strong interaction potentials acting between two quarks of different flavors in the hidden relative space between these two quarks, disregarding their electric charges and their eventual non-scalar interactions. Thus, $V_{BC}(II)$ stands for the strong potential experienced by quark*B* located at x_{II} generated by quark *C* located at x_{III}.

The Weyl spinors generate the two dimensional SL(2,C) (Special Linear Group of Rank 2, Complex) fundamental representation of the Lorentz group of transformations. The interquark interaction potential, the*V´s i*n (A1) are real scalars,

Multiply the left and right sides of these three sets of equations for *A*, *B* and *C* quarks and generalize the products into nonseparable baryon quantities according to [5, 6 (9.2.1, 2)]

$$\chi_{A\dot{b}}(I)\chi_{C\dot{h}}(III)\psi_B^f(II) \rightarrow \chi_{\dot{b}\dot{h}}^f(I,III,II)$$

$$\psi_A^c(I)\psi_C^k(III)\chi_{B\dot{e}}(II) \to \psi_{\dot{e}}^{ck}(I,III,II)$$
$$\big(V_{AB}(I)+V_{AC}(I)\big)\big(V_{CA}(III)+V_{CB}(III)\big)\big(V_{BC}(II)+V_{BA}(II)\big) \to \Phi_b(I,III,II) \quad \text{(A2)}$$

to arrive at the SSI baryon wave equations [5, 6 (9.2.3)]

$$\partial_I^{a\dot{b}}\partial_{III}^{g\dot{h}}\partial_{II\dot{e}f}\chi_{\dot{b}\dot{h}}^f(I,III,II) = -i\big(m_A m_B m_C + \Phi_b(I,III,II)\big)\psi_{\dot{e}}^{ag}(I,III,II)$$
$$\partial_{I\dot{b}c}\partial_{III\dot{h}k}\partial_{II}^{d\dot{e}}\psi_{\dot{e}}^{ck}(I,III,II) = -i\big(m_A m_B m_C + \Phi_b(I,III,II)\big)\chi_{\dot{b}\dot{h}}^d(I,III,II) \quad \text{(A3)}$$

together with $\Phi_b(I,III,II)$ satisfying a 6th order potential equation [5, 6 (9.2.9)].

As hadron data suggest that the ground state nucleon consists of a diquark [9] and a quark. Let the *u* quark *C* at x_{III} be merged into the *u* quark at $x_I$to form a *uu* diquark so that *III* drops out in (A3) and Φ_b. In this way, the practically intractable three-body quantum mechanical problem becomes a manageable two-body one.

A.2 Transformation into Laboratoryand "Hidden" Relative Space Coordinates

Following [6 (3.1.3a)], define the observable laboratory space *X* for the observable nucleon and the "hidden" relative space *x* between the quarks,

$$x^\mu = x_{II}^\mu - x_I^\mu, \qquad X^\mu = (1-a_m)x_I^\mu + a_m x_{II}^\mu \quad \text{(A4)}$$

where $a_m$is a real constant. "Hidden" variable has been proposed by Einstein, Podolsky and Rosen in 1935 and D. Bohm in 1952 in connection with quantum mechanics, well before the quark era from the 1960´s and thedominating role of such variables in SSI [4-6]. Follow the example [5,6 (3.1.5, 9)] for mesons, make the corresponding ansatz[5,6 (10.1.1)]

$$\chi_{\{\dot{a}\dot{c}\}}^e(x_I,x_{II}) = \chi_{\{\dot{a}\dot{c}\}}^e(\underline{x})\,exp\big(-iK_\mu X^\mu + i\omega_K x^0\big)$$
$$\psi_{\dot{e}}^{\{ac\}}(x_I,x_{II}) = \psi_{\dot{e}}^{\{ac\}}(\underline{x})\,exp\big(-iK_\mu X^\mu + i\omega_K x^0\big) \quad \text{(A5)}$$

where the commutator *{ab}=(ab+ba).* For rest frame baryon, $K_\mu=(E_0, \underline{K})$, where $E_0$is the baryon mass and $\underline{K}=0$, and the relative energybetween the quark and the diquark$\omega_0=0$ [5, 6 (3.1.10a), (5.7.1))], (A1) become

$$a_m = 1/2 + \omega_0/E_0 = 1/2 \;\; \text{for } K=0 \text{ and } \omega_0 = 0 \quad \text{(A6)}$$

This is the common average value for nucleons in often contact with others, like those in nuclei, chemical compounds, stars etc. An exception is that for protons in rarified interstellar hydrogen gas, where the mean collision time can be millions of years. During that long time, the invisible relative energy ω_0 can on the average be 5times the mass of the host proton and behaves like dark matter, due gravitational polarization of the diquark-quark assembly in the proton (see Figure1). Such polarization may also happen to neutrons falling inside the Schwarzschild radius of a newly formed neutron black hole and possibly prevent it from falling into a gravitational singularity, as is discussed in [6 Ch.15-16, 10 references therein]. Collisions near the outer edge of the universe may turn dark matter into dark energy causing accelerating expansion of that part of the universe.

A.3 Development of Equations of Motion of Neutron

From the 8-component wave function $\chi_{\dot{b}\dot{h}}^f$ in (A3) or the 6-component wave function $\chi_{\{\dot{a}\dot{c}\}}^e$in (A5) together with their ψcompanions, the two component spinors assigned to the ground state baryon doubletcan be extracted,

$$\chi_{01} = \frac{1}{2}\big(\chi_{\{1\dot{2}\}}^1 - \chi_{\{1\dot{1}\}}^2\big), \qquad \chi_{0\dot{2}} = \frac{1}{2}\big(\chi_{\{\dot{2}\dot{2}\}}^1 - \chi_{\{1\dot{2}\}}^2\big)$$
$$\psi_0^a = \tfrac{1}{2}\big(\psi_1^{\{12\}} - \psi_2^{\{11\}}\big), \qquad \psi_0^2 = \tfrac{1}{2}\big(\psi_1^{\{22\}} - \psi_2^{\{12\}}\big) \quad \text{(A7)}$$

Such steps turn (A3) into wave functions for ground state spin ½ baryons.

$$\partial_I^{a\dot{b}}\partial_{II}^{f\dot{e}}\partial_I^{ef}\frac{1}{2}\chi_{0\dot{b}}(x_I,x_{II}) = -i\left(M_b^3+\Phi_b(x_I,x_{II})\right)\psi_0^a$$
$$\partial_{I\dot{b}c}\partial_{II\dot{e}h}\partial_{I\dot{h}e}\frac{1}{2}\psi_0^c(x_I,x_{II}) = -i\left(M_b^3+\Phi_b(x_I,x_{II})\right)\chi_{0\dot{b}}(x_I,x_{II}) \quad \text{(A8)}$$

These steps include the replacement of the quark mass product $m_A m_B m_C$ by mass operators operating on internal or flavor functions associated with the $\chi$and ψspinors in (A8), giving rise to mass eigenvalue [6 (9.3.19)]

$$M_b^3 = \frac{1}{8}(m_A+m_B+m_C)^3 \quad \text{(A9)}$$

With (A6), (A5) turns into

$$\chi_{0\dot{b}}(x_I,x_{II}) \rightarrow \chi_{0\dot{b}}(X,x) \rightarrow \chi_{0\dot{b}}(\underline{x})\exp(-iE_0X^0 - i\omega_0 x^0) \quad \text{(A10)}$$

a similar equation for ψ_0^c (A11)

Apply the transformation [5,6 (3.1.7b)] to spherical coordinates.

$$\underline{x} = (x,y,z) = r(\hat{x},\hat{y},\hat{z}) = r\hat{r} = r(\sin\vartheta\sin\varphi, \sin\vartheta\cos\varphi, \cos\vartheta) \quad \text{(A12)}$$

Putting the total angular momentum$j$ =1/2 and orbital angular momentum l=0 leads to the decomposition [6 (10.2.3a)] and turns it into

$$\psi_0^a(\underline{x}) = \pm g_0(r)\sqrt{\pm m + {}^1\!/_2}\,Y_{0m\mp 1/2}(\vartheta,\varphi) + if_0(r)\sqrt{\mp m + {}^3\!/_2}\,Y_{1m\mp 1/2}(\vartheta,\varphi) \quad \text{(A13)}$$

where the *Y´s* are spherical harmonics, the upper signs hold for *a=1* and the lower ones for *a=2*. $\chi_{0\dot{a}}$ is found by changing the signs of $f_0(r)$. The steps after (A8)turn it into the radial equations [5,6 (10.2.12)]

$$\left[\frac{E_{0d}^3}{8} + M_b^3 + \Phi_{bd}(r) + \frac{E_{0d}}{2}\Delta_0\right]g_0(r) + \left(\frac{E_{0d}^2}{4}+\Delta_0\right)\left(\frac{\partial}{\partial r}+\frac{2}{r}\right)f_0(r) = 0$$
$$\left[\frac{E_{0d}^3}{8} - M_b^3 - \Phi_{bd}(r) + \frac{E_{0d}}{2}\Delta_1\right]f_0(r) - \left(\frac{E_{0d}^2}{4}+\Delta_1\right)\frac{\partial}{\partial r}g_0(r) = 0 \quad \text{(A14)}$$

where [5, 6 (3.1.4)] has been used.E_{0d} is the doublet baryon mass and the Δ´s are Laplace operators [5, 6 (3.4.5b)]. $\Phi_{bd}(r)$ comes from the last of (A2), where V_{AB}=$V_{BA}$and V_{CB}=$V_{BC}$are the scalar strong interaction potential between the *u* and *d* quarks dependent only upon the interquark distance *r*. The potentials V_{AC}=V_{CA}=0 because the *d* quarks *A* and *C* were to be merged into a diquark below (A3).

A.4 Strong Interaction Intraneutron Potential

The 6th order equation mentioned beneath (A3) turns into [5,6 (9.2.13b)]in which the source term on the right side drops out for rest frame baryons for which the normalization volume $\Omega\rightarrow\infty$. It now becomes

$$\Delta_0\Delta_0\Delta_0\Phi_{bd}(r) = 0, \qquad \Phi_{bd}(r) = d_b/r + d_{b0} + d_{b1}r + d_{b2}r^2 + d_{b4}r^4 \quad \text{(A15)}$$

where the d_b´s are integration constants.

These correspond to the integration constants d_m´sin [5, 6 (3.2.8a)] in the meson case. The d_m´s could be fixed from the analytical solutions for the pseudoscalar and vector mesons having the same quark content from [5, 6 (3.2.21), (5.2.2)]. This implies here that the d_b´s are to be fixed by the solutions of the two coupled third order doublet equations (A14) for *j*=1/*2* and those of the associated four coupled third orderquartet equations [5, 6 (10.5.10)] for *j*=3/2. These equations have to be solved numerically, a task beyond the scope of the present work.

To determine the d_b constants in (A15) and neutron wave functions in (A14), a less ambitious approach mentioned in [6 Ch 11] has been adopted. In [6 Ch 12], neutron beta decay was treated and the neutron life $\tau_{th}$and the asymmetry parameters A and B are given in [6 (12.6.15-17)] dependent upon the radial wave functions $g_0(r)$ and $f_0(r)$ in (A14).
(A14) has been converted into a system of 6 first order equations that are solved as an initial value problem using a Fortran program on a computer at Uppsala University. The known neutron mass is used for E_{0d} and the quarks masses determined from meson spectra in [6 Table 2] are used in (A9) for M_b. Sets of d_b values are guessed such that the radial wave functions $g_0(r)$ and$f_0(r)$converge for large r. Consider at first the d_{b4} =0 case. It turned out that once a d_{b2}<0 is chosen, the remaining d_{b1}, $d_{b0}$and $d_b$have to assume fixed values to obtain a converging solution.

Such converging solutions have been found for d_{b2} ranging at least from–0.140 to–0.975 GeV^5 in [6 Table 1] and [6 (2011) Table 1]. However, only the d_{b2} =–0.3202 case led to the correct neutron life of τ_{th}=880 sec. and asymmetry parameters$A$= –0.1218 and B=0.9794, close to PDG data A= – 0.1184 and B=0.9807[6 Table.1]. Thus, [6 (2011) Table.1] shows that for d_{b2} = –0.1621, τ_{th}=38 sec. and d_{b2} = –0.4042, τ_{th}=3349 sec.
Turning to the $d_{b4}\neq0$ case, [6 §11.1.4] points out that the corresponding converging solution [6 Table.2] leads to τ_{th}, A and B values in disagreement with PDG data.

Therefore, adopt the neutron case in [6 Table 1]

$$d_{b4} = 0, d_{b2} = -0.3202 \text{ GeV}^5, \quad d_{b1} = 2.272 \text{ GeV}^4, \quad d_{b0} = -4.922 \text{ GiV}^3, \quad d_b = 1.024 \text{ GeV}^2 \text{(A16)}$$

A.5 Neutron Radial Wave Functions

The associated wave functions have been plotted in [6 Figure 6b] and earlier in [5 (2011) Figure7] and are reproduced in Figure A1.

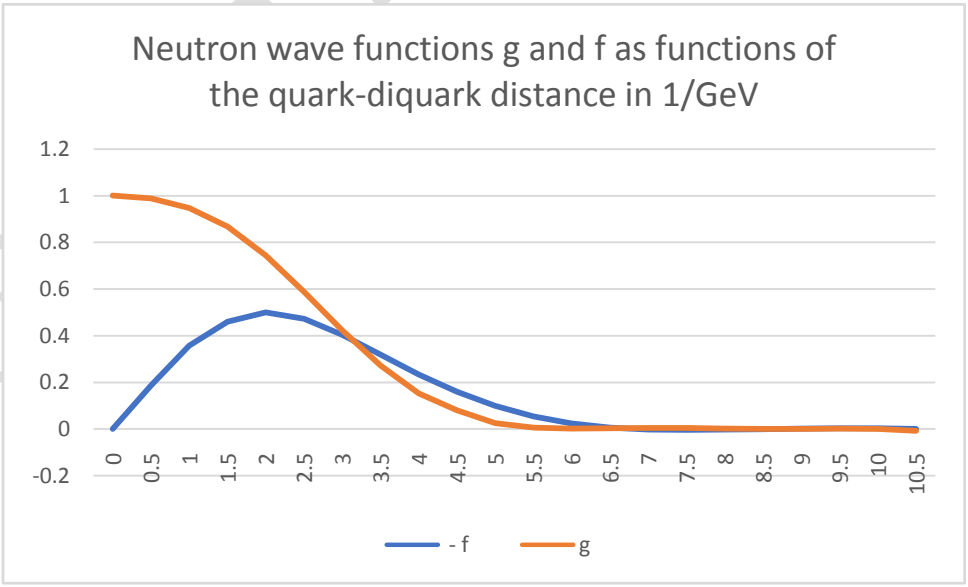

Figure A1. Radial neutron wave functions in (A14). The horizontal length unit is GeV^{-1} = 1.24 fm.

The average distance r_a between the *dd* diquark and the *u* quark in the hidden relative space$\underline{x}$ is

obtained from Figure A1 via [6 (12.6.22)]

$$r_a = \frac{\int d\underline{x}^3 r\left(\left(\chi_{0\dot{b}}(\underline{x})\right)^* \chi_{0\dot{b}}(\underline{x}) + \left(\psi_0^a(\underline{x})\right)^* \psi_0^a(\underline{x})\right)}{\int d\underline{x}^3\left(\left(\chi_{0\dot{b}}(\underline{x})\right)^* \chi_{0\dot{b}}(\underline{x}) + \left(\psi_0^a(\underline{x})\right)^* \psi_0^a(\underline{x})\right)} = \frac{\int dr\, r^3\left(g_0^2(r) + f_0^2(r)\right)}{\int dr\, r^2\left(g_0^2(r) + f_0^2(r)\right)} = 3.05 \text{ fm} \quad \text{(A17)}$$

A.6 Universal Strong *u* – *d* Interaction Potential

The *u* – *d* quark strong interaction potential [6 (12.6.18)], also seen in the third of (A2), is

$$V_s(r) = \left|\frac{\Phi_{bd}(r)}{2}\right|^{1/3}, \quad V_s(r = 0.288 \text{ fm}) = 0 \quad \text{(A18)}$$

which can be found from (A15) with (A16) and is plotted in Figure A2.

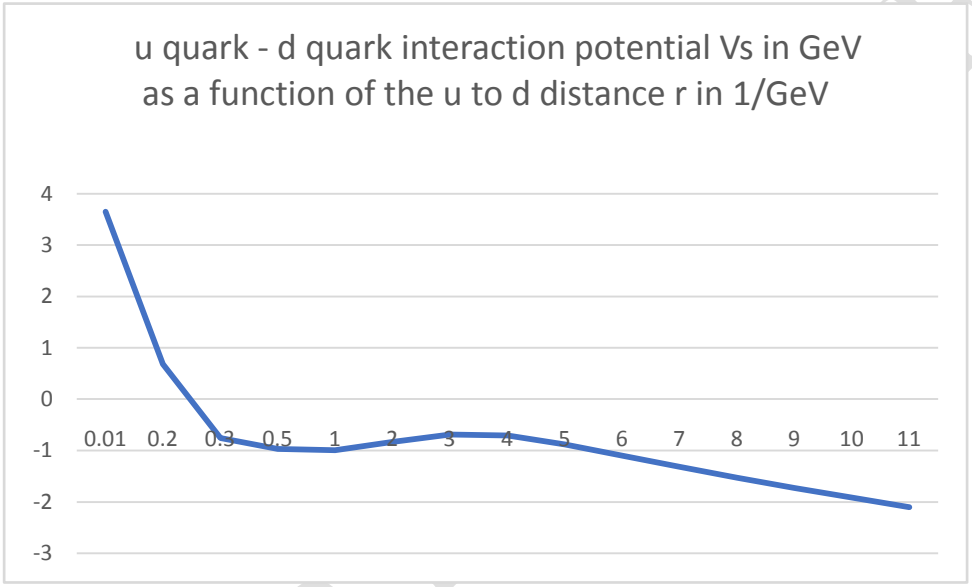

Figure A2. Interquark potential $V_s(r)$ (A18). Thehorizontallength unitGeV^{-1}=1.24 fm. This scale has been amplified in the r<1GeV^{-1}region.

This strong interaction potential bears some resemblance to the internucleon Reid potential from 1968 [2 Nuclear Force]. Both are repulsive at small separations and approach +∞ at 0 separation but turn into attractive potential wells at larger separations. The scales are different. The Reid potential is internucleon and empirical in the laboratory space while V_s in Figure A2 is interquark in the hidden relative space between quarks and theoretical, as required by the convergence of the radial nucleon wave functions in Figure A1.

Theresults in this Appendix derived from neutron properties also hold approximately for the proton because the differences in mass and quark masses between these two nucleons are only fractions of 1 %. These are independent of the quark charges, which can be switched off without affecting the results in this Appendix. This is seen in e. g. the radial equations (A14) which do not contain quark charge.

The dominant confining term d_{b2}= –0.3202 $\propto r^2$appears also to be reminiscent to the 3-dimensional harmonic potential employed in the "shell" model.

REFERENCES.

[1] Burgess, C. and Moore, G. (2007) The Standard Model, A Primer, Cambridge Univ. Press
[2] Wikipedia 2023
[3] ATLAS, CMS Collaboration 2012 Phys Lett B716 1, 30.

[4] Hoh, F. C. (1993,1994) *Int. J. Theoretical Physics*, **32,** 1111|, **33,** 2325
[5] Hoh, F.C. (2011) Scalar Strong Interaction Hadron Theory, (2019) II, Nova Science Publishers, New York
[6] Hoh, F.C. (2022) Scalar Strong Interaction Hadron Theory III, Nova Science Publishers, New York
[7] Spyrou, A.; Kohley, Z.; Baumann, T.; Bazin, D.; et al. (2012). [7*doi*:*10.1103/PhysRevLett.108.102501*. *PMID* *22463404*.
[8] Corson, E. M. (1953) Introduction to Tensors, Spinor and Relativistic Wave Equations, Blackie and Sons, Ch. 2
[9]Lichtenberg, D. B.; Namgung, W.; Predazzi, E. and Wills, J. G. (1982)*Physical Review Letters*. **48** (24):1653-1656
[10] Hoh, F. C. (2021) *Int. Astronomy and Astrophysics Research***3 (3):** 49-61 Article no.IAARJ. 80374 open access at https://www.journaliaarj.com/index.php/IAARJ/article/view/48